

Table S1: Primer and siRNA sequences

Gene	Sequence (5'-3')	
Bax	F: CCCGAGAGGTCTTTTCCGAG	R: CCAGCCCATGATGGTTCTGAT
Bcl2	F: GGTGGGGTCATGTGTGTGG	R: CGGTCAGGTACTCAGTCATCC
GXP4	F: GAGGCAAGACCGAAGTAAACTAC	R: CCGAACTGGTTACACGGGAA
HO-1	F: AAGACTGCGTTCCTGCTCAAC	R: AAAGCCCTACAGCAACTGTCTG
Nrf2	F: GGTTGGCCCTTTCCTGCTTTATA	R: CCCTTGACAGCACAGAAGAGAAT
Piezo1	F: ACTCCGCACTCATCAAGTGG	R: CAGCAGGAGAAAGTCGCTGA
HLA-A	F: TTCTGGAGAGGAGCAGAGATACA	R: CTATCTGAGCTCTTCCTCCTCCA
β -actin	F: CATGTACGTTGCTATCCAGGC	R: CTCCTTAATGTCACGCACGAT
Piezo1-siRNA	S: CCAAGUACUGGAUCUAUGU	AS: ACAUAGAUCCAGUACUUGG

F: Forward; R: reverse; S: sense; AS: antisense

Figure S1

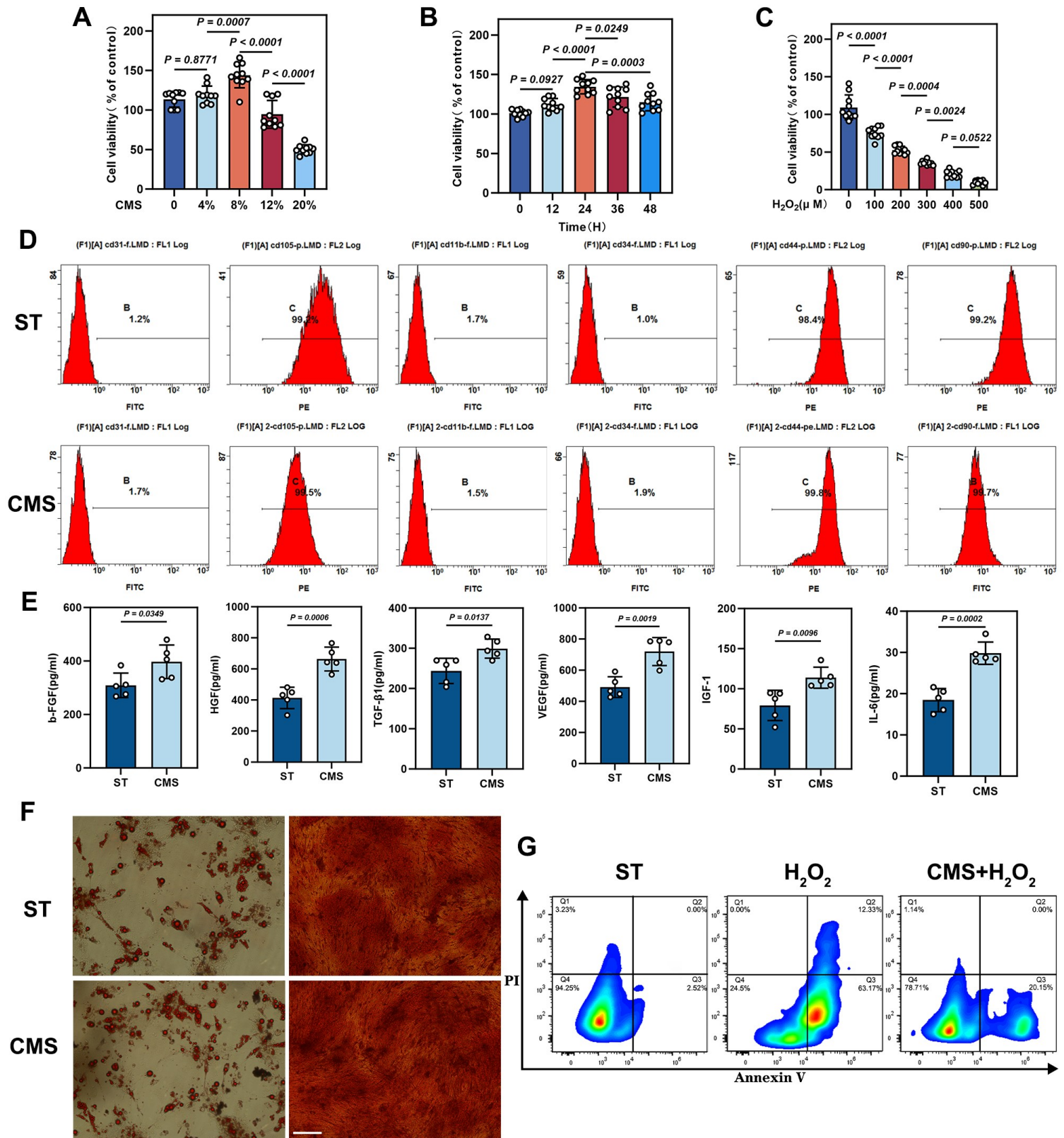


Fig. S1. Effects of Cyclic Mechanical Stretch (CMS) and oxidative stress on viability, phenotype, paracrine function, and apoptosis of adipose-derived stem cells (ADSCs).

(A) Cell Counting Kit-8 (CCK-8) proliferation assay of ADSCs subjected to varying mechanical strain amplitudes (0%, 4%, 8%, 12%, 20%) (n=10). (B) CCK-8 assay assessing ADSC proliferation after CMS for different durations (12 h, 24 h, 36 h, 48 h) (n=10). (C) H₂O₂ dose-response curve (0, 100, 200, 300, 400, 500 μ M; 24 h) showing ADSC viability assessed via CCK-8 assay (n=10). (D) Flow cytometry identification of surface markers for ADSCs cultured under static conditions (ST) and after CMS. (E) Comparison of paracrine secretion profiles of ADSCs under CMS or ST conditions (n=5). (F) Representative images comparing adipogenic and osteogenic differentiation potential of ADSCs under CMS or ST conditions (Scale bar = 275 μ m). (G) Apoptosis analysis of ADSCs assessed by flow cytometry using Annexin V/PI staining. (Data are presented as mean \pm standard deviation).

Figure S2

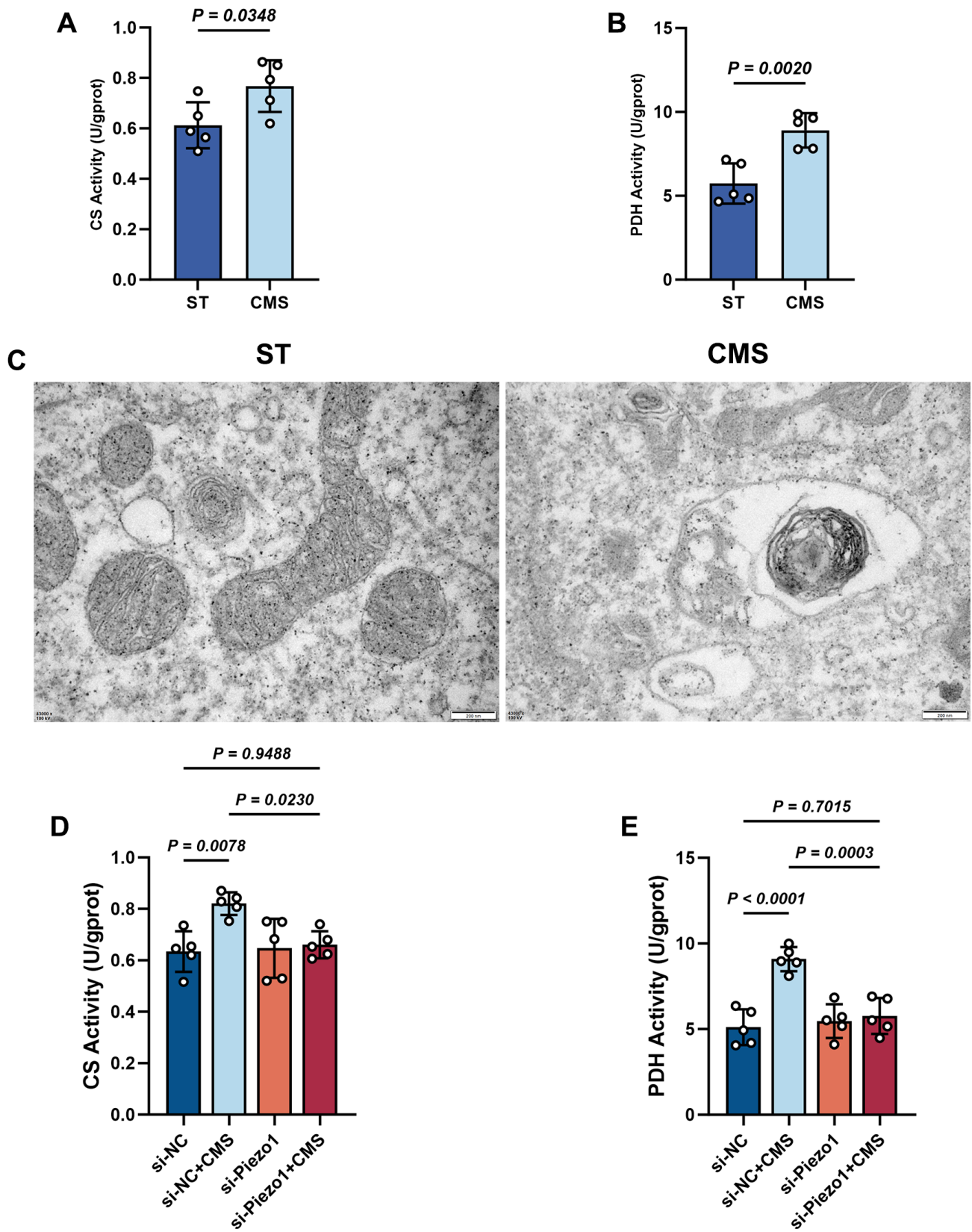


Fig. S2. Effects of CMS and Piezo1 Knockdown on Citrate Synthase (CS) and Pyruvate Dehydrogenase (PDH) Levels in ADSCs

(A-B) CS and PDH levels in ADSCs cultured under CMS versus ST (n=5).

(C) Transmission electron microscopy images of mitochondrial ultrastructure (n=5). (D-

E) CS and PDH content in ADSCs following Piezo1 knockdown (n=5). (Data are presented as mean \pm standard deviation).

Figure S3

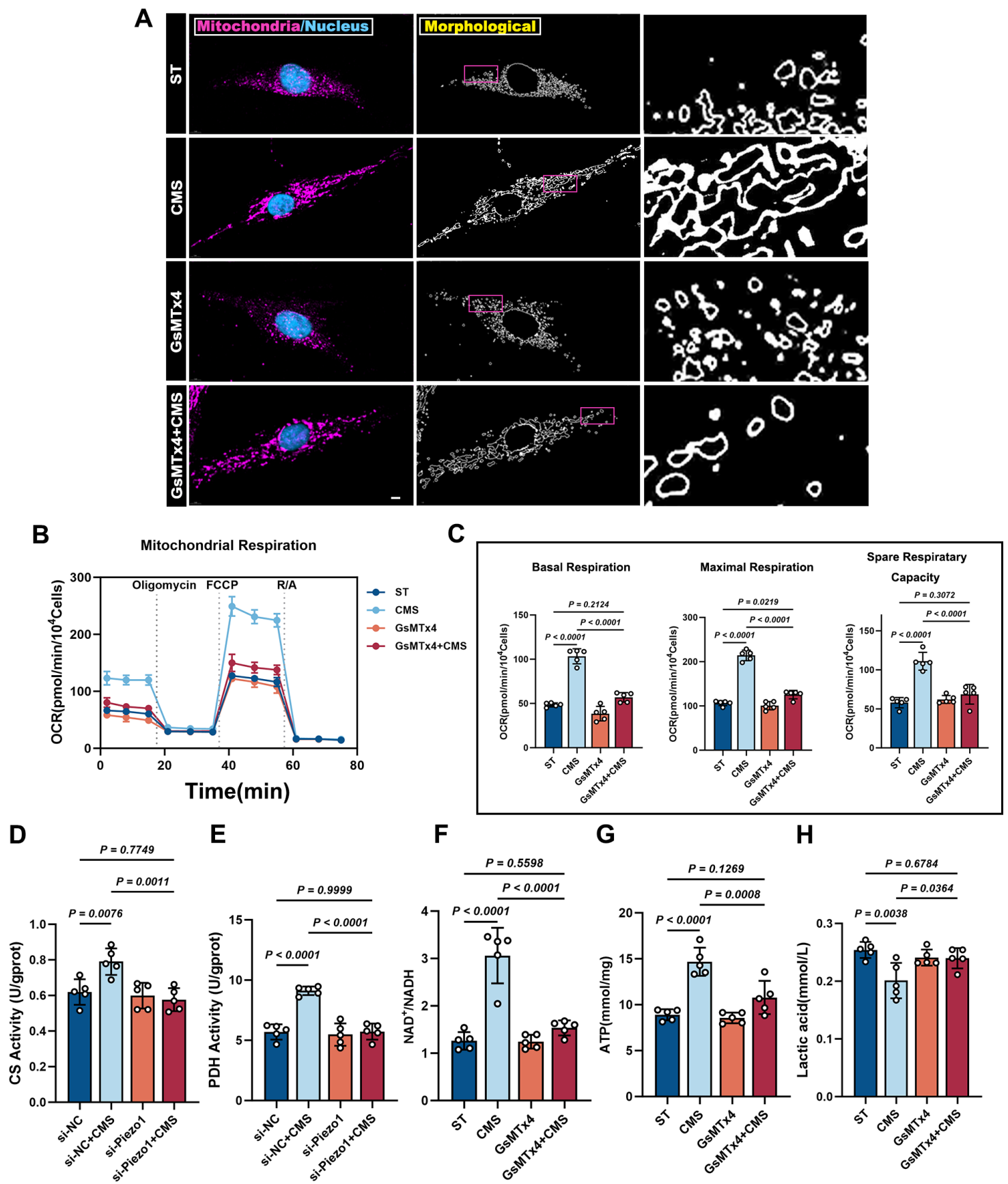


Fig. S3. Effect of Piezo1 inhibitor GsMTx4 on mechanical stimulation-enhanced ADSCs mitochondrial dynamics and mitophagy.

(A) Cultured ADSCs were labeled with MitoTracker Red and Hoechst 33342, and mitochondrial morphological changes were observed using confocal microscopy in the presence of the Piezo1 inhibitor GsMTx4 (Scale bar = 5 μ m). (B-C) Representative traces of OCR assay ADSCs in the presence of the Piezo1 inhibitor GsMTx4 (n=5). (D-H) CS, PDH, ATP, NAD⁺NADH, MAD and FRAP levels in ADSCs in the presence of the Piezo1 inhibitor GsMTx4 (n=5). (Data are presented as mean \pm standard deviation).

Figure S4

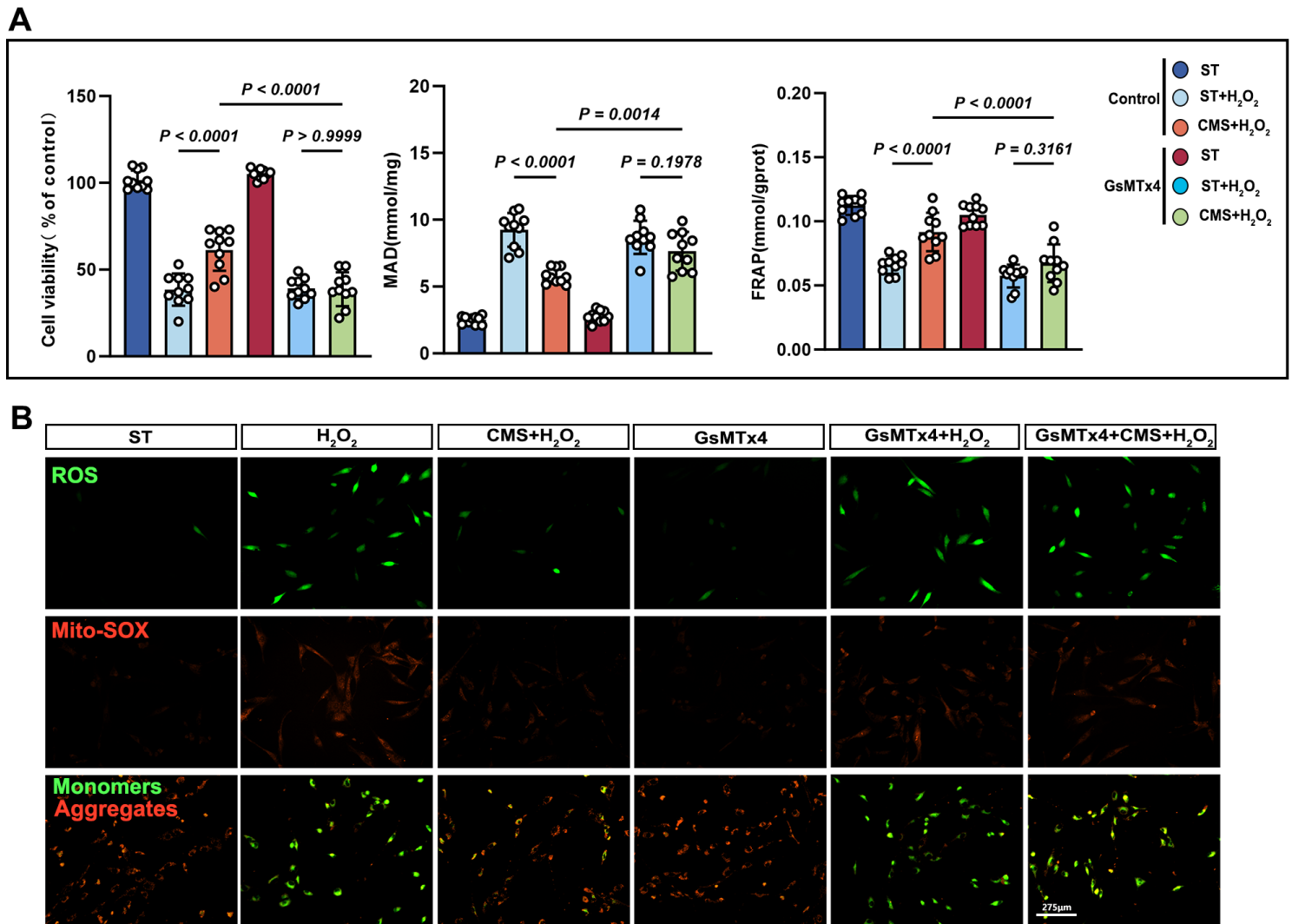


Fig. S4. Effect of Piezo1 inhibitor GsMTx4 on mechanical stimulation-enhanced survival and mitochondrial homeostasis of ADSCs under oxidative stress.

(A) CCK-8 assay and measurements of malondialdehyde and ferric reducing antioxidant power levels were conducted in the presence of the Piezo1 inhibitor GsMTx4 (n=10). (B) ROS levels (DCFH-DA/Mito-SOX) and mitochondrial membrane potential (JC-1, red: J-aggregates/green: monomers) were assessed by fluorescence imaging, with the red/green ratio quantifying $\Delta\Psi_m$, in the presence of the Piezo1 inhibitor GsMTx4 (Scale bar = 275 μm). (Data are presented as mean \pm standard deviation).